

# Electrical conduction mechanism and dielectric properties of vanadium doped ZnTe thin films

M. S. HOSSAIN\*, R. ISLAM<sup>a</sup>, K. A. KHAN<sup>a</sup>

*Departments of Physics, Rajshahi University of Engineering & Technology (RUET), Rajshahi-6204, Bangladesh*

*<sup>a</sup>Departments of Applied Physics & Electronic Engineering, University of Rajshahi, Rajshahi-6205, Bangladesh*

ZnTe:V (contains 2.5 to 10wt% V) thin films with various thicknesses have been prepared onto glass substrate by e-beam technique at a pressure  $\sim 8 \times 10^{-4}$  Pa. The dc conductivity  $\sigma_{dc}$ , indicates a thermally activated carrier hopping; it increases with increasing temperature. Ac conductivity  $\sigma_{ac}(\omega)$ , of the prepared thin films has been measured in the frequency range 0.04 to  $10^4$  kHz, over the temperature range 303 to 383 K, respectively. Obtained data reveal that  $\sigma_{ac}(\omega)$  obey the relation,  $\sigma_{ac}(\omega) = A\omega^S$  and the exponent S is found to decrease by increasing temperature. The values of S of the investigated thin films lie between  $0.57 \leq S \leq 0.91$ . The obtained experimental results of ac conductivity have been analyzed with reference to various theoretical models. The analysis shows that the correlated barrier-hopping (CBH) model is the dominant conduction mechanism for the electron transport in the vanadium doped ZnTe films. Application of the CBH model reveals that the electronic conduction takes place via bipolaron or mixed polaron hopping process in the whole temperature range of the study. Both the dielectric constant and dielectric loss showed a decrease with increasing frequency while they increased with increasing temperature.

(Received May 18, 2007; accepted June 27, 2007)

*Keywords:* ZnTe:V thin films, E-beam technique, Electrical conduction mechanism, Dielectric properties

## 1. Introduction

Zinc Telluride (ZnTe) is a II-VI family of compound semiconductors, which has recently been focused of great interest due its low cost and high optical absorption coefficient for application to photovoltaic and photoelectrochemical cells [1-4]. Literature [5] reports that ZnTe exhibits improved photorefractive response when it is doped with vanadium. The combination of photorefractivity and semiconductivity makes this material attractive for use in a variety of applications including optical power limiting, holographic interferometry, optical computing and optical communication [5, 6]. Studies of electronic nature of amorphous material give information about its electrical behavior and this may be related to structural properties. ZnTe:V is a kind of wide band gap amorphous material, which exhibits unique electrical properties and infrared transmission [5-7]. The disorder in atomic configuration is responsible for the localized electronic states within the material. The conductivity of semiconducting glasses is known to be frequency dependent, which as expected is due to conduction in the localized state. Since the charge carriers are localized, ac technique is a powerful experimental method often employed to probe their behavior [8-10].

The ac conductivity  $\sigma_{ac}(\omega)$ , of amorphous semiconductors is usually expressed as

$$\sigma_{ac}(\omega) = \sigma_T - \sigma_{dc} = A\omega^S \quad (1)$$

where  $\omega$  is the angular frequency of the applied field, A is a constant,  $S(\leq 1.0)$  is frequency exponent,  $\sigma_T$  is the total conductivity including the frequency dependent conductivity under ac field and  $\sigma_{dc}$  is the dc conductivity

[11-16]. This equation is valid for several low mobility amorphous and even crystalline materials [17]. Measurement of ac conductivity of semiconductors has been extensively used to understand the conduction process [12] and it is also a powerful tool for obtaining information about the defect states in amorphous semiconductors [18]. Various models have been proposed by several investigators to explain the behavior of the frequency exponent S, in the case of semiconducting glasses [18-25]. The Quantum-Mechanical Tunneling (QMT) model was the first of charge transfer for doped Si, proposed by Pollak and Geballe [19] and Austin and Mott [25] then applied it to amorphous semiconductors. According to QMT, it assumes that there is no lattice distortion associated with carrier whose motion gives rise to the ac conductivity and the frequency exponent S, is predicted to be temperature independent but frequency dependent (i.e. S decreases with increasing frequency). The correlated barrier-hopping (CBH) model proposed by Elliott [12, 22] has been applied to the glassy semiconductors. In this model, correlated barrier hopping of bipolarons (i.e. two electrons hopping between charge defects  $D^+$  and  $D^-$ ) has been proposed to interpret the frequency dependence of conductivity in amorphous glasses as given in Eq. 1. The theory has explained many low temperature features, particularly the dependence of A and S parameters on temperature. However, it does not explain the high temperature behavior so well, in low frequency range. Shimakawa [23, 24] suggests that at high temperature  $D^0$  states are produced by thermal excitation of  $D^+$  and /or  $D^-$  states, and that single polaron hopping (i.e. one electron hopping between  $D^0$  and  $D^+$  or  $D^-$  and a hole between  $D^0$  and  $D^-$ ) becomes dominant process.

Dielectric relaxation studies are important in understanding the nature and the origin of dielectric losses, which, in turn, may be useful in the determination of structure and defects in solids. The dielectric behavior of thin film devices depends not only on their material properties, but also on the substrate used for fabrication and the type of the metal electrodes. Fringing effects at the edges of thin film dielectrics are usually negligible because the thickness of the dielectric is usually very small compared to its lateral dimensions. The magnitude of geometric and measured capacitance may differ if the electric field at the metal insulator interface varies with the insulator over the region.

To our knowledge, no report is available on the study of dc and or ac conduction mechanisms and dielectric properties of vanadium doped ZnTe films. Combining dc and ac measurements at various temperatures is certainly of great importance in order to obtain a better understanding of the occurring electrical transport mechanism. In this paper, we present the results of dc, ac conductivity and dielectric properties measurement performed in amorphous vanadium doped ZnTe thin films having various compositions of 2.5 to 10wt% V as a function of frequency and temperatures, respectively and discusses these results in terms of the above-mentioned transport models. The concept of CBH model, incorporating the suggestions made by Shimakawa [23] is applied to author's data.

## 2. Experimental

Vanadium doped ZnTe thin films have been prepared onto glass substrate by electron bombardment heating technique in vacuum (Coating Unit; Edwards Vacuum Ltd, Model: E306) at a pressure of  $4 \times 10^{-4}$  Pa, from a mixture of ZnTe powder (99.999% pure) and vanadium powder (99.999% pure) obtained from Aldrich Chemical Company, USA. The composite of ZnTe:V (contains 2.5 to 10wt% V) films were deposited at a rate of  $2.05 \text{ nms}^{-1}$  to a thickness of 100 to 250 nm, respectively. The effective area of the films was about  $0.28 \times 10^{-4} \text{ m}^2$ . Fig. 1 shows the schematic diagram of the deposited ZnTe:V sandwiched films. Metal Aluminum (Al) thick film was evaporated onto glass substrate as a base electrode followed by the ZnTe:V sample and finally the second (Al) film as top electrode was evaporated. The films were sandwiched between two Aluminum electrodes of thickness 150 nm, which act as ohmic contacts with ZnTe:V films.

For dc conductivity measurement, a 15V dc fixed bias was maintained. A power supply (Heathkit, Model: IP-2717A) was used to pass a constant dc current through the test sample. An electrometer (Keithley, Model: 614) was used to monitor the current through the sample and a digital multimeter (Model: DM-206) was used to measure the potential differences across each sample. The glass substrate was heated by a specially designed heater and the temperature was measured by a chromel-alumel thermocouple placed on the middle of the substrate. Annealing was performed at a temperature of 473 K for

duration of 3 hours in air. The thickness was measured by the Tolansky [26] interference method with an accuracy of  $\pm 5 \text{ nm}$ .

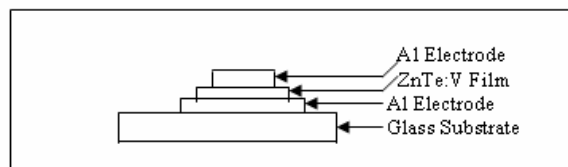


Fig. 1. Schematic diagram of sandwich Al/ZnTe:V/Al film.

A HP 4294A Programmable Automatic LCZ meter manufactured by Agilent Technologies, Japan, Ltd., was used for the ac measurements. The ohmic behavior has been checked before the measurements. Ac conductivity  $\sigma_{ac}(\omega)$ , of the investigated thin films was obtained in the frequency range 0.04 to  $10^4$  kHz, over the temperature range 303 to 383 K, respectively.

The structure of ZnTe:V thin film of various compositions (2.5 to 10wt% V) and of thicknesses 100 to 250 nm, respectively for both as-deposited and annealed films were examined by X-ray diffraction (XRD) technique using the monochromatic  $\text{CuK}\alpha$  radiation made by apparatus, RINT 2200, Rigaku, Japan. Peak intensities were recorded corresponding to  $2\theta$  values. Fig. 2 shows the intensities of XRD spectra of a 150 nm thick ZnTe:V as-deposited sample of composition 2.5wt% V. Examination of a number of XRD spectra of various as-deposited vanadium doped ZnTe thin films indicates that there is no remarkable peak in the spectra and it hints that the material is an amorphous one. The annealed ZnTe:V thin film of various thicknesses was also examined by XRD technique and the sample exhibits no noticeable peaks, indicating it an amorphous in nature.

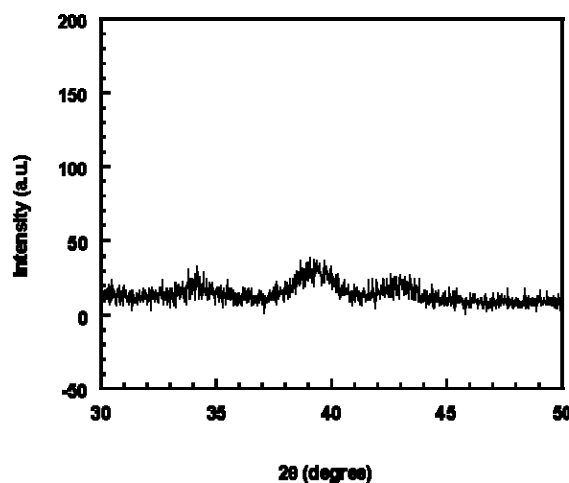


Fig. 2. XRD pattern for a 150 nm thick ZnTe:V film doped with 2.5wt% V.

### 3. Results and discussion

#### 3.1. Temperature dependence of dc conductivity

In general for a semiconducting material, dc conductivity increases exponentially with temperature indicating that the conductivity is a thermally activated process. Mathematically, it can be expressed by the well-known Arrhenius relation as

$$\sigma_{dc} = \sigma_o \exp(-\Delta E / kT) \quad (2)$$

where  $\sigma_o$  is called pre-exponential factor,  $\Delta E$  is called the activation energy,  $T$  is the absolute temperature and  $k$  is Boltzmann constant. These parameters are of significance to differentiate the nature of various conduction mechanisms. Fig. 3 shows temperature dependence of dc conductivity  $\sigma_{dc}$ , for a 150 nm thick vanadium doped ZnTe thin films of compositions 2.5 to 10wt% V, respectively. From the figure, it is clear that the dc conductivity  $\sigma_{dc}$ , varies exponentially with temperature, as  $\ln \sigma_{dc}$  vs.  $1000/T$  curves are straight lines. Such behavior is consistent with Eq. 2. The values of electrical parameters  $\Delta E$  and  $\sigma_o$  are listed in Table 1.

**Table 1. Ac and dc electrical parameters for a 150 nm thick ZnTe:V films of dopant composition 2.5wt% V.**

Frequency, $f$ (KHz)	Activation energy, $\Delta E$ (eV)	Pre-exponential factor, $\sigma_o$ ( $\Omega^{-1}\cdot\text{m}^{-1}$ )	Conductivity, $\sigma$ at 303 K ( $\Omega^{-1}\cdot\text{m}^{-1}$ )
0 (dc)	0.81	$8.29 \times 10^{-10}$	$1.54 \times 10^{-12}$
1	0.29	$2.05 \times 10^{-10}$	$2.94 \times 10^{-11}$
10	0.27	$2.35 \times 10^{-9}$	$2.24 \times 10^{-10}$
100	0.20	$1.62 \times 10^{-8}$	$2.67 \times 10^{-9}$

A low value of  $\sigma_o$  indicates the presence of contribution of localized states and the conduction occurs by phonon-assisted hopping between the localized states. The electrical conduction of the films follows a mechanism in which the electron or hole hops from one localized site to the next. Whenever it is transferred to another site, the surrounding molecules respond to this perturbation with structural changes and the electron or hole is temporarily trapped in the potential well leading to atomic polarization. The electron resides at this site until it is thermally activated to migrate to another site [14, 27]. Another aspect of this charge hopping mechanism is that the electron or hole tends to associate with local defects. So, the activation energy for charge transport may also include the energy of freeing the hole from its position next to the defects [28, 29].

#### 3.2. Temperature and frequency dependence of ac conductivity

The dependence of ac conductivity  $\sigma_{ac}(\omega)$ , on temperature is also obey the well-known relation of Eq. 2. Fig. 4 shows the ac conductivity as a function of reciprocal

temperature for a 150 nm ZnTe:V thin films at a particular frequency of 10 kHz produced at four compositions of 2.5, 5.0, 7.5 and 10 wt% V, respectively. From these plots the activation energies  $\Delta E$ , and the pre-exponential factors  $\sigma_o$ , have been calculated for three frequencies of 1, 10 and 100 kHz, respectively and their values are given in Table 1. As it is observed from this Table, the activation energy decreases with increasing frequency. The low value of the ac activation energy and the increase of  $\sigma_{ac}(\omega)$ , with the increase of frequency confirm that hopping conduction is the dominant current transport mechanisms [14]. Thus, the increase of the applied frequency enhances the electronic jumps between the localized states; consequently, the activation energy  $\Delta E$ , decreases with increasing frequency.

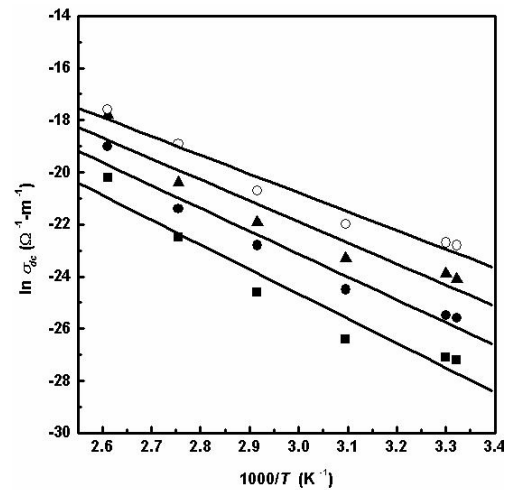


**Fig. 3.  $\ln \sigma_{dc}$  vs.  $1000/T$  for a 150 nm thick ZnTe:V film of composition ( $\blacksquare$  2.5wt% V,  $\bullet$  5.0wt% V,  $\blacktriangle$  7.5wt% V and  $\circ$  10wt% V).**

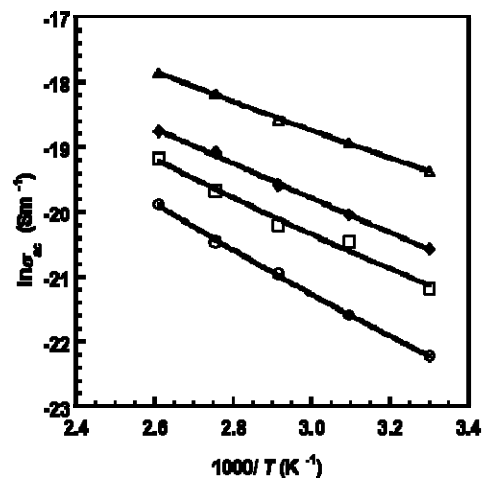


**Fig. 4.  $\ln \sigma_{ac}$  vs.  $1/T$  for a 150 nm thick ZnTe:V film at a fixed frequency of 10 kHz ( $\circ$  2.5 wt% V,  $\square$  5.0 wt% V,  $\diamond$  7.5wt% V,  $\Delta$  10wt% V).**

The total conductivity  $\sigma_T(\omega)$ , at a particular angular frequency,  $\omega$  and at a certain temperature can be expressed

by Eq. 1 [17,18]. It is noted that Eq. 1 is valid when the ac and dc conductivities arise from completely separate mechanisms; otherwise the dc conductivity represents the ac conductivity in the limit  $\omega \rightarrow (0)$  [12].

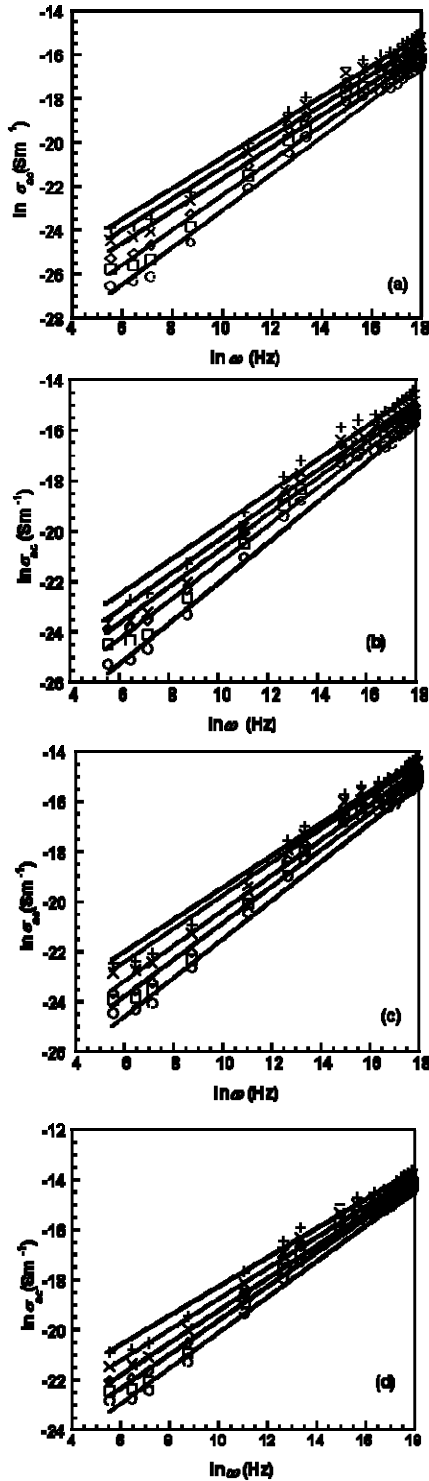


Fig. 5.  $\ln \sigma_{ac}$  vs.  $\ln \omega$  for a 150 nm thick ZnTe:V film of composition a) 2.5wt% V, b) 5.0wt% V, c) 7.5 wt% V and d) 10wt% V ( $\circ$  303,  $\square$  323,  $\diamond$  343,  $\times$  363,  $+$  383 K).

The frequency dependence of ac conductivity  $\sigma_{ac}(\omega)$ , for a 150 nm thick ZnTe:V (contains 2.5 to 10wt% V) thin films has been measured in the frequency range of 0.04 to  $10^4$  kHz, over the temperature range of 303 to 383 K, respectively. The dependence of  $\ln \sigma_{ac}(\omega)$  vs.  $\ln(\omega)$  for a 150 nm thick ZnTe:V film for four compositions of 2.5, 5.0, 7.5 and 10wt% V, respectively are shown in Fig. 5. It is clear from these curves that the ac conductivity  $\sigma_{ac}(\omega)$ , has a frequency dependence given by the following relation [12]

$$\sigma_{ac}(\omega) = A \omega^S \quad (3)$$

where A is a constant depending on temperature,  $\omega$  is the angular frequency and S is an exponent, generally less than or equal to unity. It is also clear that the variation in the logarithmic ac conductivity is almost linear with the variation in logarithmic frequency and that  $\sigma_{ac}(\omega)$ , increases with increasing both frequency and temperature. The frequency exponent S is obtained by the least squares straight-line fit of the experimental data and it is plotted in Fig. 6 for a film of ZnTe:V at various dopant compositions of 2.5 to 10wt% V, respectively. The exponent S decreases as the temperature increases. The observed frequency dependence of  $\ln \sigma_{ac}$  reveals that the mechanism responsible for ac conduction could be due to hopping [22, 30, 31].

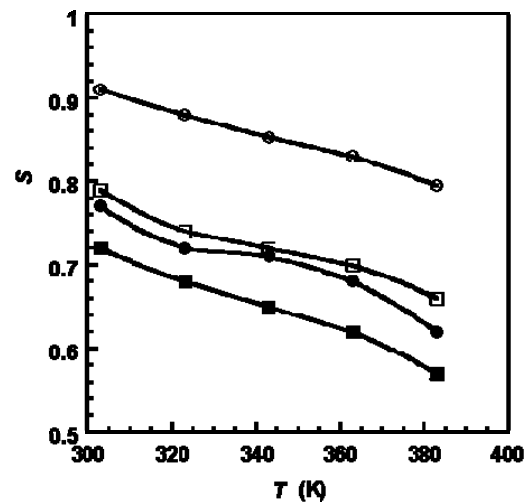


Fig. 6. Frequency exponent S vs. T for a 150 nm thick ZnTe:V film at various compositions ( $\circ$  2.5 wt% V,  $\square$  5.0 wt% V,  $\bullet$  7.5 wt% V,  $\blacksquare$  10 wt% V).

In order to explain the behavior of  $\sigma_{ac}(\omega)$ , with both temperature and frequency, different theoretical models have been proposed to co-relate the conduction mechanism of ac conductivity with S(T) behavior [32]. Theories proposed for ac conduction in amorphous semiconductors [25, 33, 34] have mostly assumed that carrier motion occurs through quantum mechanical tunneling (QMT) between localized states near the Fermi-level. For the QMT model, the frequency exponent S, is temperature independent but frequency dependent. This conclusion is further strengthened from the S vs. T plot in

Fig. 6. It is observed in Fig. 6 that  $S$  decreases from a value of 0.91 to 0.57 with increasing temperature in contrast with the QMT model, which predicts a temperature independent of  $S$  [12].

The temperature dependence of  $S$  can be compared in the tunneling models if the carrier forms a small or large polaron. The small polaron tunneling model (SPT) [17, 18] is also not suitable mechanism for explaining the results of author's sample because it predicts an increase of  $S$  with the increase of temperature, in sharp contrast with the experimental observation shown in Fig. 6. The large polaron-tunneling (LPT) model is also not applicable for the present film studied, since this model predicts a minimum in the temperature dependence of  $S$ , which is not observed in Fig. 6. In the classical hopping over a barrier (HOB) model [18, 20], the value of frequency exponent  $S$  is 1, and this rules out the applicability of this model to the ZnTe:V film system.

We now, invoke the correlated barrier-hopping (CBH) model to explain the observed behavior in Fig. 6. In the CBH model, the electrons in charged defects states hop over the coulomb barrier, the height of which is given as,

$$W = W_m - (ne^2/\pi\epsilon_1\epsilon_0R) \quad (4)$$

where  $n$  is the number of polarons involved in the hopping process ( $n = 1, n = 2$  for single and bipolaron hopping process, respectively),  $e$  is the electronic charge,  $R$  is the distance between the hopping sites,  $\epsilon_1, \epsilon_0$  are the dielectric constants of the material and free space, respectively and  $W_m$  is the maximum barrier height (for a bipolaron  $W_m$  is approximately equal to the band gap width).

The relaxation time,  $\tau$  for electrons to hop over a barrier of height  $W$  is given by

$$\tau = \tau_0 \exp(W/kT) \quad (5)$$

where  $\tau_0$  is the characteristic relaxation time, which is of the order of an atomic vibrational period. In the pair approximation model, a major contribution to the ac conductivity arises from hopping within the pairs of sites for which  $\omega\tau = 1$ .

According to the CBH model [12, 18, 35, 36], the ac conductivity can be expressed as

$$\sigma_{ac}(\omega) = n\pi^3 N^2 \epsilon_1 \epsilon_0 \omega R_\omega^6 / 24 \quad (6)$$

where  $N$  is the density of localized states at which carriers exist. The temperature dependence of  $\sigma_{ac}(\omega)$  originates from the hopping length  $R_\omega$ , in Eq. 6, where

$$R_\omega = (ne^2/\pi\epsilon_1\epsilon_0)/[W_m + kT\ln(\omega\tau_0)] \quad (7)$$

The frequency dependence of  $\sigma_{ac}(\omega)$  in this model arises from the factor  $\omega R_\omega^6$ . The temperature dependence of the frequency exponent  $S$  arises due to the temperature dependence of  $R_\omega$  and is evaluated to be

$$S = 1 - 6kT/[W_m + kT\ln(\omega\tau_0)] \quad (8)$$

Thus, in the CBH model a temperature dependent exponent  $S(T)$ , is predicted, with  $S$  decreasing as the temperature increases and  $S$  increasing towards unity as the temperature tends to zero, in marked contrast to the QMT or simple HOB mechanism. The temperature dependence on  $S$ , shown in Fig. 6 is consistent with Eq. 8, indicating the dominance of a CBH model as a transport mechanism for author's vanadium doped ZnTe thin films. The values of  $N^2$  and the maximum barrier height  $W_m$ , are adjusted to fit the calculated curves with the experimental results using Eq. 6. The fitting is done at particular frequency of 10 kHz and the same values of the parameters are used for other frequencies. The various parameters used in the fitting procedures are summarized in Table 2.

Table 2. Ac electrical conductivity parameters obtained by fitting the experimental data to the correlated barrier hopping (CBH) model for ZnTe:V films.

Composi tions (wt%V)	$S$	$W_m$			$R$			$N$			$W$ (eV)	$\tau$ (sec) $\times 10^{-3}$
		(eV) $n=1$	(eV) $n=2$	(eV) $n=3$	$\times 10^{-3}$ $n=1$	$\times 10^{-3}$ $n=2$	$\times 10^{-3}$ $n=3$	( $m^{-3} eV^{-1}$ ) $n=1$	( $m^{-3} eV^{-1}$ ) $n=2$	( $m^{-3} eV^{-1}$ ) $n=3$		
2.5	0.91	1.12	2.23	3.35	1.54	1.11	1.01	$1.93 \times 10^{23}$	$2.13 \times 10^{24}$	$2.80 \times 10^{24}$	0.49	1.59
5.0	0.79	0.62	1.24	1.86	7.21	2.45	2.00	$1.32 \times 10^{21}$	$5.04 \times 10^{23}$	$8.33 \times 10^{23}$	0.49	1.59
7.5	0.77	0.59	1.17	1.76	9.30	2.57	2.07	$6.38 \times 10^{20}$	$2.48 \times 10^{23}$	$5.14 \times 10^{23}$	0.49	1.59
10	0.72	0.53	1.05	1.58	24.06	2.85	2.21	$2.27 \times 10^{20}$	$6.74 \times 10^{23}$	$1.46 \times 10^{24}$	0.49	1.59

Fig. 7 shows the CBH model fittings of the calculated values of the ac conductivity  $\sigma_{ac}(\omega)$  dependence on inverse temperature with the experimental results. The fitting was done at 10 kHz considering the hopping process of single polaron, bipolaron and mixed polaron ( $n = 1, 2$  and  $3$ , respectively) for a 150 nm thick ZnTe:V thin films produced at various dopant compositions. It is seen from the fitting curves that for a single polaron system ( $n=1$ ) the calculated values seems to be far off from the experimental result for all four dopant compositions,

whereas the fittings at ( $n = 2$  and  $3$ , respectively) for bipolaron and /or mixed polaron case, the calculated values of ac conductivity do in fair agreement with the respective experimental results. Similar fittings of CBH model have also been done for a particular 150 nm thick ZnTe:V thin films of composition 2.5wt% V at various frequencies of 1, 10 and 100 kHz, respectively and these results of the fitting is shown in Fig. 8. It is also seen from these curves that for the case of bipolaron and /or mixed polaron ( $n = 2$  and  $3$ , respectively) the agreement between

the calculated values of conductivity with the experimental observation are very close. The above results, therefore, suggests that the fitting is reasonably good, indicating that the conduction mechanism may be caused due to bipolaron or mixed polaron hopping process.

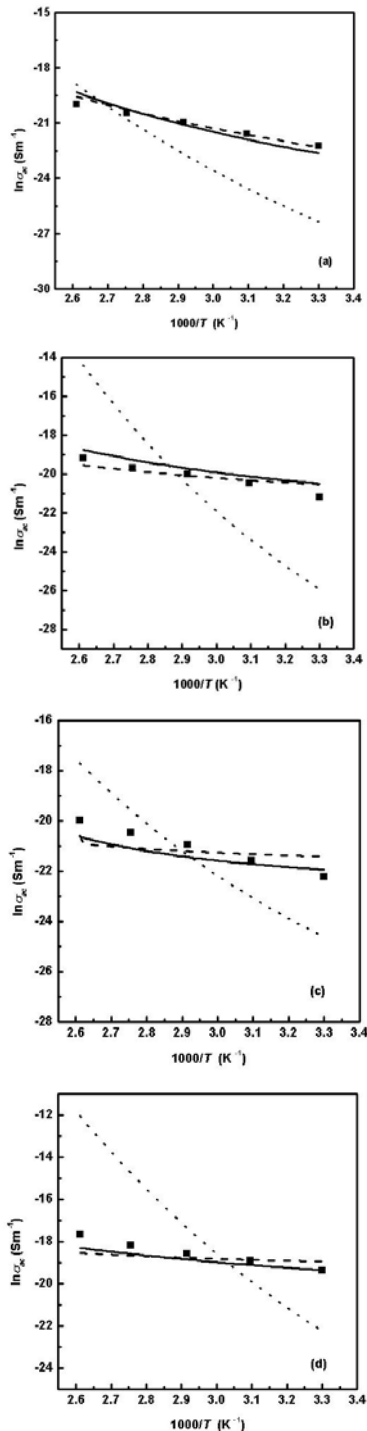


Fig. 7.  $\ln \sigma_{ac}$  vs.  $1000/T$  for a 150 nm thick ZnTe:V film of composition a) 2.5wt% V, b) 5.0wt% V, c) 7.5wt% V and d) 10wt% V (■ Experimental result; Calculated results: ..... single polaron, — bipolaron and - - - mixed polaron).

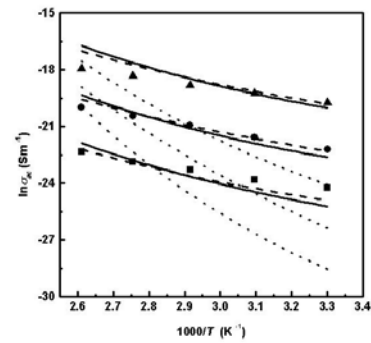


Fig. 8.  $\ln \sigma_{ac}$  vs.  $1000/T$  for a 150 nm thick ZnTe:V film of dopant composition 2.5wt% V (Experimental results: ■ 1 kHz, ● 10 kHz and ▲ 100 kHz; Calculated results: ..... single polaron, — bipolaron and - - - mixed polaron).

### 3.3. Dielectric properties

The temperature and frequency dependence of dielectric constant  $\epsilon_1$ , and dielectric loss  $\epsilon_2$ , are studied for film samples in the temperature range 303–383 K and frequency range 0.1–100 kHz. The results for a composition 2.5 wt% V are shown in Figs. 9 and 10, respectively. A comparative study of these figures is indicates that  $\epsilon_1$  and  $\epsilon_2$  increase with the increase of temperature (the increase being different at different frequencies) and they decrease with increasing frequency. This type of behavior has also been reported in semiconducting films [11, 14, 27]. The variation of  $\epsilon_1$  with the temperature is related to the charge carriers which in most cases cannot orient themselves with respect to the direction of the applied field: therefore, they possess a weak contribution to the polarization and the dielectric constant  $\epsilon_1$ . As the temperature increases, the bound charge carriers get enough thermal excitation energy to be able to respond to the charge in the external field more easily. This in turn enhances their contribution to the polarization leading to an increase of the dielectric constant  $\epsilon_1$  of the sample [37]. When the frequency is increased, the dipoles will no longer be able to rotate sufficiently rapidly, so their oscillation will begin to lay behind this field, which explains the observed decrease in  $\epsilon_1$  with frequency.

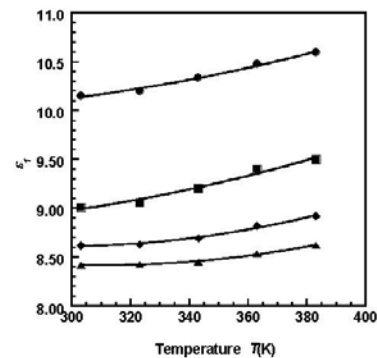


Fig. 9.  $\epsilon_1$  vs.  $T$  for a 150 nm thick ZnTe:V film of dopant composition 2.5wt% V at various frequencies (● 0.1, ■ 1, ◆ 10, ▲ 100 kHz).

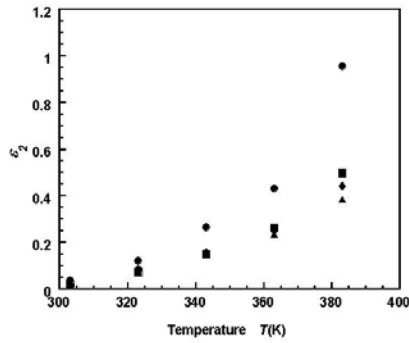


Fig. 10.  $\epsilon_2$  vs.  $T$  for a 150 nm thick ZnTe:V film of dopant composition 2.5wt% V at various frequencies ( $\bullet$  0.1,  $\blacksquare$  1,  $\blacklozenge$  10,  $\blacktriangle$  100 kHz).

It is shown that the dielectric loss  $\epsilon_2$ , increases as the temperature increases for the considered frequencies; at low temperature, this increase is linear and the variation of  $\epsilon_2$  with frequency is small, this linear region extending to higher values of temperature with increasing frequency, while at higher frequencies, it increases nonlinearly. This behavior can be clarified by plotting  $\ln(\epsilon_2)$  versus  $\ln(\omega)$  for various temperatures as shown in Fig. 11. It is observed that a series of straight lines with different slopes is obtained, in which  $\epsilon_2$  decreases as the frequency increases and it increases as the temperature increases.

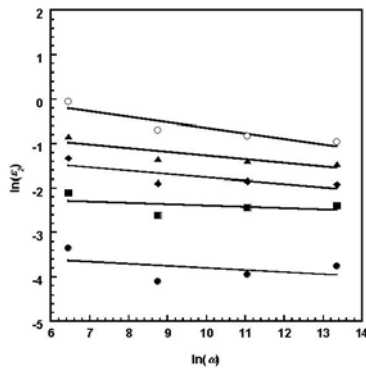


Fig. 11.  $\ln(\epsilon_2)$  vs.  $\ln(\omega)$  for a 150 nm thick ZnTe:V film of composition 2.5 wt% V at various temperatures ( $\bullet$  303,  $\blacksquare$  323,  $\blacklozenge$  343,  $\blacktriangle$  363,  $\circ$  383 K).

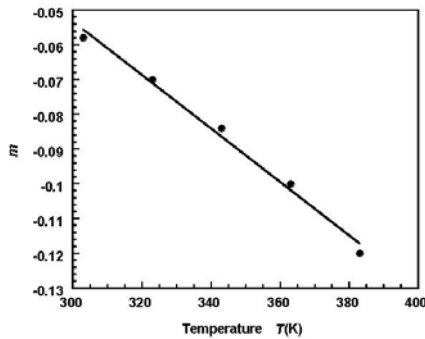


Fig. 12. Parameter  $m$  vs.  $T$  for a 150 nm thick ZnTe:V film of composition 2.5 wt% V.

The frequency dependence of  $\epsilon_2$  follows the relation [38]

$$\epsilon_2 = (\epsilon_s - \epsilon_\infty) 2\pi^2 N (ne^2 / \epsilon_s)^3 kT \tau_o^m W_M^{-4} \omega^m \quad (9)$$

According to the proposed theory,  $\epsilon_2$  should follow a power law with frequency, i.e.

$$\epsilon_2 = G\omega^m \quad (10)$$

with

$$m = -4kT/W_M \quad (11)$$

where  $W_M$  is the barrier height  $\epsilon_s$  is the static dielectric constant,  $\epsilon_\infty$  is the dielectric constant at infinite frequency,  $G$  is a constant depending on temperature and the other symbols have the same meaning as before.

The power  $m$ , is calculated from the slopes of the curves of Fig. 11 and it was found that the values of  $m = -0.058$  (at 303 K) are negative and it decreases linearly with increasing temperature as shown in Fig. 12; this is in agreement with the prediction of the theory. For this value of parameter  $m$ ,  $W_M$  is 1.80 (eV) and with the help Eq. 8,  $S \approx 0.91$ . The parameter  $m$ , confirms the observed variations as a function of the measuring temperature. In fact, this result is satisfying if we consider the empirical law [39, 40]:  $\sigma_{ac}(\omega) = \omega\epsilon_2(\omega) = A\omega^S$ . It is obvious that if  $S$  is temperature dependent [11, 35, 36],  $m$  should consequently depend on  $T$ .

#### 4. Conclusions

ZnTe:V thin films (contains 2.5 to 10wt% V) with various thickness have been produced onto glass substrate by e-beam technique at a pressure  $\sim 8 \times 10^{-4}$  Pa. The dc conductivity  $\sigma_{dc}$ , of the ZnTe:V films exhibits a thermally activated carrier hopping. The measurement of ac conductivity  $\sigma_{ac}(\omega)$ , in the frequency range of 0.04 to  $10^4$  kHz, over a temperature range of 303 to 383 K were done for a ZnTe:V films of various dopant compositions. Obtained data reveal that  $\sigma_{ac}(\omega)$  obeys the relation  $\sigma_{ac}(\omega) = A\omega^S$ , where  $S$  is the frequency exponent and its value lies between  $0.57 \leq S \leq 0.91$ . The experimental results of ac conductivity  $\sigma_{ac}(\omega)$ , have been analyzed in terms of various theoretical models. Application of correlated barrier-hopping (CBH) model reveals that electronic conduction takes place by bipolaron or mixed polaron hopping process. It is, therefore, concluded that the combined mechanism of single polaron and bipolaron hopping or bipolaron hopping satisfactorily accounts for the ac conductivity of Vanadium doped Zinc Telluride system. The different temperatures obtained from the fits of this model of the experimental data are reasonable. The values of dielectric constant  $\epsilon_1$ , and dielectric loss  $\epsilon_2$ , increase with increasing temperature and with decreasing frequency. Values of the maximum barrier height were estimated from the data of dielectric loss, and are the good agreement with the theory of hopping of charge carriers over a potential barrier between charged defect states. The

value of the barrier height  $W_M$ , is calculated according to the Giuntini et al. model [38].

### Acknowledgements

Authors gratefully acknowledge the assistance in measuring the XRD and Transmittance data by Dr. M. Shahjahan in Japan. One of the authors M. S. Hossain is indebted to Rajshahi University of Engineering & Technology, Bangladesh for providing the study leave during this work.

### References

- [1] A. Z. Nozik, R. Memming, *J. Phys. Chem.* **100**, 13061 (1996).
- [2] J. O. M. Bockris, K. Uosaki, *J. Electrochem. Soc.* **124**, 1348 (1997).
- [3] K. K. Mishra, K. Rajeshwar, *J. Electrochem. Soc.* **273**, 169 (1978).
- [4] D. Ham, K. K. Mishra, K. Rajeshwar, *J. Electrochem. Soc.* **138**, 100 (1991).
- [5] M. Ziari, W. H. Steier, P. M. Ranon, *Appl. Phys. Lett.* **60**, 1052 (1992).
- [6] W. M. B. Duval, NASA Lewis Research Center, Commercial Technology Office, Attn: Tech. Brief Patent Status, Technical support Package (TSP), Lew-16498, Cleveland, Ohio, U. S. A.
- [7] M. S. Hossain, R. Islam, K. A. Khan, Proc. 10th Asian Conf. on Solid State Ionics, Kandy, Sri Lanka, Ed. B. V. R. Chowdari, M. A. Careem, M. A. K. L. Dissanayake, R. M. G. Rajapakse, V. A. Seneviratne, Imperial College Press, Singapore, 2006, p. 154.
- [8] A. N. Sreeram, A. K. Varshneya, D. R. Swiler, *J. Non-Cryst. Solids* **130**, 225 (1991).
- [9] A. Rahman, P. C. Mahanta, *Thin Solid Films* **66**, 125 (1979).
- [10] S. P. Fu, Y. F. Chen, *J. Appl. Phys.* **93**, 2140 (2003).
- [11] M. I. Mohammed, A. S. Abd-rabo, E. A. Mahmoud, *Egypt. J. Sol.* **25**, 49 (2002).
- [12] S. R. Elliott, *Advances in Physics* **36**, 135 (1987).
- [13] M. Fadel, S. S. Fouad, *J. Materials Science* **36**, 3667 (2001).
- [14] M. M. El-Nahass, H. M. Zeyada, M. M. El-Samanoudy, E. M. El-Menyawy, *J. Phys.: Condens. Mater* **18**, 5163 (2006).
- [15] A. K. Jonscher, *Nature* **267**, 673 (1977).
- [16] N. Mehta, D. Kumar, S. Kumar, A. Kumar, *Chalcogenide Letters* **2**, 103 (2005).
- [17] N. F. Mott, E. A. Davis, *Electronic Processes in Non-Crystalline Materials*, Clarendon press, Oxford (1979).
- [18] A. R. Long, *Adv. Phys.* **31**, 553 (1982).
- [19] M. Pollak, T. H. Geballe, *Phys. Rev.* **B 122**, 1742 (1961).
- [20] M. Pollak, G. E. Pike, *Phys. Rev. Lett.* **28**, 1449 (1972).
- [21] X. Lecleac'h, *J. Physique* **40**, 27 (1979).
- [22] S. R. Elliott, *Phil. Mag.* **B 36**, 1291 (1977).
- [23] K. Shimakawa, *Phil. Mag.* **46**, 123 (1982).
- [24] A. Ganjoo, A. Yoshida, K. Shimakawa, *J. Non-Cryst. Solids* **198-200**, 313-317 (1998).
- [25] L.G. Austin, N. F. Mott, *Adv. Phys.* **18**, 41 (1969).
- [26] S. Tolansky, *Multiple Beam Interferometry of Surfaces and Films*, Oxford University Press, London (1948).
- [27] F. Yakuphanoglu, Y. Aydogdu, U. Schatzschneider, E. Rentschler, *Solid State Commun.* **128**, 63 (2003).
- [28] D. F. Shriver, P. W. Atkins, C. H. Langford, *Inorganic Chemistry*, Freeman, New York (1994).
- [29] K. F. Purcell, J. C. Kotz, *Inorganic Chemistry*, Philadelphia, Saunders (1977).
- [30] R. D. Gould, A. K. Hassan, *Thin Solid Films* **223**, 334 (1993).
- [31] M. M. El-Desky, K. Tahoon, M. Y. Hassaan, *Materials Chemistry and Physics* **69**, 180 (2001).
- [32] S. Hazara, A. Chosh, *Phil. Mag.* **B 74**, 235 (1996).
- [33] M. Pollak, *Phil. Mag.* **23**, 519 (1971).
- [34] C. A. Hogarth, M. H. Islam, S. S. M. S. Rahman, *J. of Materials Science* **28**, 518 (1993).
- [35] S. R. Elliott, *Phil. Mag.* **37**, 553 (1978).
- [36] S. R. Elliott, *Phil. Mag.* **B 36**, 1291 (1977).
- [37] M. R. Anantharaman, S. Shindhu, S. Jagatheesan, K. A. Molini, P. Kurian, *J. Phys. D: Appl. Phys.* **32**, 1801 (1999).
- [38] J. C. Giuntini, J. V. Zanchetta, D. Jullien, R. Eholie, P. Houenou, *J. Non-Cryst. Solids* **45**, 57 (1981).
- [39] R. M. Hill, A. K. Jonscher, *J. Non-Cryst. Solids* **32**, 53 (1979).
- [40] K. L. Ngai, A. K. Jonscher, C. T. White, *Nature* **277**, 185 (1979).

\*Corresponding author: sazzad\_phy@yahoo.com